Ground-based hyperspectral remote sensing for weed management in crop production

Yanbo Huang[1*], Matthew A. Lee[2], Steven J. Thomson[3], Krishna N. Reddy[1]

(1. *United States Department of Agriculture, Agricultural Research Service, Crop Production Systems Research Unit, PO Box 350, Stoneville MS 38776, USA*;

2. *Department of Electrical and Computer Engineering, Mississippi State University, Mississippi State MS 39762, USA;*

3. *United States Department of Agriculture, National Institute of Food and Agriculture, Washington DC 20024, USA)*

Abstract: Agricultural remote sensing has been developed and applied in monitoring soil, crop growth, weed infestation, insects, diseases and water status in farm fields to provide data and information to guide agricultural management practices. Precision agriculture has been implemented through prescription mapping of crop fields at different scales with the data remotely sensed from space-borne, airborne and ground-based platforms. Ground-based remote sensing techniques offer portability, flexibility and controllability in applications for precision agriculture. In weed management, crop injury from off-target herbicide spray drift and herbicide resistance in weeds are two important issues. For precision weed management, ground-based hyperspectral remote sensing techniques were developed for detection of crop injury from dicamba and differentiation between glyphosate resistant and sensitive weeds. This research presents the techniques for ground-based hyperspectral remote sensing for these two applications. Results illustrate the advantages of ground-based hyperspectral remote sensing for precision weed management.

Keywords: ground-based remote sensing, hyperspectral, crop injury, herbicide resistance, precision agriculture

DOI: 10.3965/j.ijabe.20160902.2137

Citation: Huang Y, Lee M A, Thomson S J, Reddy K N. Ground-based hyperspectral remote sensing for weed management in crop production. Int J Agric & Biol Eng, 2016; 9(2): 98－109.

1 Introduction

Agricultural remote sensing has been developed and applied for observation of crop fields for soil variability, crop growth status, crop stress from weeds, pests, nutrition, and water deficiencies to provide prescription data to guide precision operations[1-5]. Remote sensing for precision agriculture provides observation at the field scale to map within-field variability with high-resolution data for effective prescription of variable-rate equipment[4,6]. Remote sensing systems and methods can be effective and versatile to provide timely data for precision agriculture.

Weed management is an important part of crop production. Traditional weed management was conducted based on manual crop field monitoring and sampling, which is expensive, laborious and time-consuming. Remote sensing has provided an approach to rapid acquisition of spatial data over crop fields for timely decision support to improve weed management in crop production[7,8]. In recent years with the development of sensor and transducer technologies, remote sensing has been improved for weed sensing and control, especially with hyperspectral sensing and

Received date: 2015-09-01 **Accepted date:** 2016-03-09

Biographies: Matthew A. Lee, Post-doctoral, research associate, research interest: image processing and pattern recognition, Email: lee@ece.msstate.edu; **Steven J. Thomson**, National Program Leader, research interest: aerial application technology and remote sensing, Email: steven.j.thomson@nifa.usda.gov; **Krishna N. Reddy**, Supervisory Research Plant Physiologist, research interest: weed biology and management, Email: krishna.reddy@ars.usda.gov.

***Corresponding author: Yanbo Huang**, Research Agricultural Engineer, research interest: application technology, remote sensing, soft computing and process control. Mailing address: P.O. Box 350, 141 Experiment Station Road, Stoneville MS 38776, USA. Tel: +1-662-686-5354, Email: yanbo.huang@ars.usda.gov.

imaging[9-11].

Remote sensing systems are typically on the platforms of satellites, aircraft and ground on-the-go vehicles. This research focused on the ground-based systems and hyperspectral techniques we have developed and applied in the past few years. Ground-based remote sensing offers portability, flexibility and controllability compared to space-borne and airborne remote sensing. For precision weed management, we have developed cost-effective ground-based hyperspectral remote sensing (GBHRS) systems and methods for detection analysis of crop injury from dicamba and differentiation between glyphosate resistant and sensitive weeds. This research presents the techniques of GBHRS we have developed for these two applications. The results illustrated the advantages of GBHRS for precision weed management.

2 GBHRS platforms and sensors

GBHRS has various platforms for laboratory and field studies. The laboratory platform is used for studies of greenhouse plants and plant leaves sampled from the field with controlled illumination and fixed leaf sample position under the sensor. The field platform is used for studies of plant canopy in the field that must account for uncertainties of sun light intensity, sun angle, and wind. The sensors typically used include a non-imaging spectroradiometer and multispectral and hyperspectral cameras. We have configured hyperspectral non-imaging and imaging sensors for laboratory and field studies. However, wind interference was a challenge when implementing a field on-the-go line-scan hyperspectral imaging system.

2.1 Handheld spectroradiometer

We used the FieldSpec 2 handheld spectroradiometer (ASD Inc., Boulder, CO, USA) to rapidly measure plant canopy in the field to provide visible-near infrared (VNIR) spectral sensing of plants. The measuring range of the spectroradiometer is 325-1075 nm, with spectral resolution of 3 nm within the range of 350-1000 nm of which is in our concern for plant sensing in the VNIR bands. The spectral sampling interval was 1 nm. The plant reflectance, R, is calculated with the following equation:

$$R = \frac{I_s - I_d}{I_w - I_d} \times R_w \quad (1)$$

where, I_s is the radiance of the measured plant; I_w is the radiance of the white reference; I_d is the radiance of dark current of the spectroradiometer; R_w is the reflectance of the white reference from the calibration file provided by the factory of the white reference. The white reference was a 0.3×0.3 m Spectrolon® white reference board (Labsphere, North Sutton, GH, USA) with nominal reflectance of 99%.

2.2 Hyperspectral imaging system in laboratory

The Resonon Pika II hyperspectral camera (Resonon, Bozeman, MT) was used for hyperspectral imaging in the laboratory. The laboratory system mounts the camera on a stand to capture images. The Pika II system is a push-broom hyperspectral sensor with a spectral range of 400-900 nm in 240 wavelength bands. An objective lens with a 23 mm focal length gives the camera a 12° field of view. Typically, the camera is held about 66 cm above the plants, which results in a spatial resolution at about 0.24×0.24 mm/pixel. The high spatial resolution permits a large number of pure plant pixels to be collected and analyzed.

The camera stand is modeled after a carpenter's sawhorse with a linear motor attached to the cross bar of the sawhorse. The camera is attached to the linear actuator, which is used to move the camera in a linear scanning motion during imaging. The sample is placed below the camera and illuminated by a pair of 70 watt quartz-tungsten-halogen illuminator reflectance lamps, which integrated a reflector to produce stable illumination over the 350 nm to 2500 nm range (ASD Inc., Boulder, CO), located at opposite ends of the crossbar holding the camera and linear motor.

Light condition is an important consideration in a laboratory setting, and it is difficult to get proper configuration. The main issue with light condition is uneven light intensity. This is because the light intensity from most illumination sources is angle and to a lesser extent time dependent. The time dependency typically occurs when the lights are initially turned on and dampens after the lights and electronics heat up. However, if the lights utilize alternating current, they may

constantly flicker, which will result in a striped illumination pattern in an image acquired using a pushbroom type sensor. Thus, it is important to use direct current with illumination sources and let the illumination sources have enough time to stabilize before collecting data. The angle dependency of the light intensity is more difficult to solve however. Typically illuminators have the highest intensity along the beam axis and reduce in intensity as the angle from the beam axis increases. In spite of the uneven light intensity, if the sample is approximately two dimensional in shape, and can be laid flat on the stage for imaging, then precise reflectance measurements can be obtained through sensor calibration. This requires that white reference and dark reference images be taken, and the mean spectrum from each reference is used for calibration. However, if the sample is three dimensional, then the light in the entire view frustum must be considered. Most likely it will be impossible to get the light intensity even in three dimensions. In order to minimize the lighting intensity variability, we directed the lights so the beam axes from the lights crossed about 60 cm above the sample stage that one light focused in front of the other on the sample stage (Figure 1). We also found it beneficial to image plants of approximately the same size and shape. This resulted in more consistent illumination of the samples.

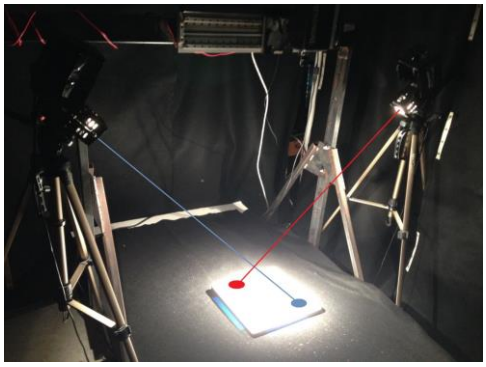

Figure 1 Lights beam crossing on about 60 cm above the sample stage for hyperspectral imaging

2.3 On-the-go hyperspectral imaging system

When deployed in the on-the-go configuration for field study, the camera mount is attached to the 3-point hitch behind a standard tractor. This provides a very secure connection between the camera and the tractor, and allows the camera height and pitch to be adjusted on the go using the tractor hitch. The camera mount uses the same crossbar that is on the laboratory stand, and attaches to a pole (Figure 2). The camera mount functions similarly to the laboratory function. However, precautions have to be taken because of environmental conditions to avoid water from rain or irrigation systems being exposed on the camera and electronics at all cost. Fortunately, the best imaging conditions are found on cloudless days between 10:00 am and 2:00 pm, so rain is not typically an issue. However, high temperatures can be encountered in these conditions. Based on experience, we have determined that there is an issue with the electronics overheating in the linear actuator. When it gets too hot, the linear actuator stops working. The solution we have found is to blow compressed air on the electronics components of the motor to cool them off. Typically, the procedure restores function within 30 seconds, so it is not an issue as far a data collection is concerned. When the hyperspectral camera gets hot, the amount of thermal noise in the charged coupled device (CCD) sensor increases and alters the sensitivity of the camera. In order maintain the calibration, a white and dark reference is collected each time an image is collected. These two values (along with the image of the plant canopy) are used to compute reflectance of the plants using Equation (1).

Figure 2 Field on-the-go system hyperspectral imaging system.

Another issue encountered when measuring plant canopy in the field is wind interference, which causes the plants to move during image scanning to have images with twisted plant shapes. This makes visual identification of plants difficult due to distortion of plant morphology in the images. However, the spectral signature of the plants can still be extracted for spectral analysis if the background can be removed from the vegetation. If there are no other plants in the image, and

the background is bare soil (as is common in agricultural fields), no additional procedures need to be taken in the field because the spectrum of soil is very different from the spectrum of plants. In cases where there may be other plants in the background, we place a non-reflective black felt sheet around the plant to act as the background. The spectrum of felt is also very different from the spectrum of plants (Figure 3), so it is easy to segment the plant pixels in the image. In the data analysis, once all the plant pixels are labeled, they are used to compute the mean spectral signature of the plant.

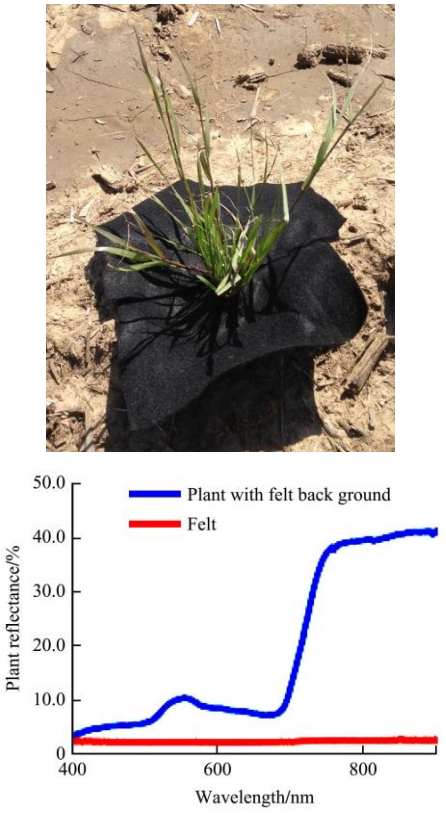

Figure 3 Placement of felt around the target weed and the spectral curves of the plant and the felt

3 Applications

3.1 Detection and characterization of crop injury from dicamba herbicide

3.1.1 ASD handheld spectroradiometer for in-field early detection of soybean injury from dicamba

In January 2015, USDA announced deregulation of Monsanto's Roundup Ready 2 Xtend™ soybean (the first industrial biotech-stacked soybean trait with both dicamba and glyphosate herbicide tolerance) and Bollgard II® XtendFlex™ cotton (the first triple stack herbicide-tolerance technology in cotton, with tolerance to dicamba, glyphosate and glufosinate herbicides) (Monsanto Company, St, Louis, MO). The Roundup Ready 2 Xtend Crop System is an advanced weed management tool in the fight against glyphosate-resistant and tough-to-control broadleaf weeds in soybeans and cotton. Although the launch of dicamba-resistant trait cotton and soybean is still pending approval of new dicamba formulations by USEPA (U.S. Environmental Protection Agency, Washington DC), off-target dicamba drift from routine use in dicamba-resistant crops onto susceptible crops has been a concern. In Mississippi, there was one dicamba drift complaint in each of the years, 2012 and 2013 (Source: John Campbell, Bureau of Plant Industry, MS Dept. Agriculture and Commerce). It can be predicted that with the adoption of the Roundup Ready 2 Xtend Crop System in the near future the concern would be much more with significantly increased complaints.

Remote sensing provides a cost-effective approach to detect changes in canopy spectral properties in crop injury from off-target herbicide spray. We have assessed crop injury from the off-target of aerially applied glyphosate using aerial color-infrared (CIR) imagery for cotton[12] and soybean[13]. However, early detection of the injury before appearance of visible injury symptoms is needed for farmers to prevent yield losses. Our previous studies have shown that hyperspectral reflectance measurements can be used to detect glyphosate injury of soybean earlier than appearance of visible injury symptoms[14,15]. The purpose of the study is to characterize hyperspectral reflectance properties of soybean treated with and without dicamba and investigate the parameters from in-field measured hyperspectral data for early detection of soybean injury from simulated low-dose dicamba drift.

For the study, a 4.5 hm^2 field in USDA-ARS Crop Production Systems Research Farm in Stoneville, Mississippi (central latitude: 33.445062° and central longitude: −90.869967°) was buffered by corn plants to isolate the vapor drift of dicamba. In the east side of the field 32 plots were planted soybean (Progeny P4819LL) on May 7, 2014. Each plot consisted eight rows with 0.97 m wide and 24 m long. In the 32 plots 4 blocks

were formed with 8 plots in each. Due to too many weeds in the most southern block, analysis was on the other three blocks. So, the experimental design was a randomized complete block design with 3 replications with plot treatments, 0.0X (control), 0.05X and 0.1X where, X=0.56 kg ae/hm^2 of dicamba. On June 17, 2014, six weeks after soybean planting and soybean at 5-trifoliolate to 6-trifoliolate leaf stage, dimethylamine salt of dicamba, RIFLE® (Loveland Products, Inc., Greeley, CO) was applied using a tractor mounted sprayer with Tee Jet 4003 standard flat-spray nozzles delivering 140 L/hm^2 of water at 193 kPa. No postemergence herbicides were applied up to 3 weeks after dicamba treatment for taking various measurements. Three weeks after dicamba treatment, other postemergence herbicides were applied as needed to keep the plots weed-free, and the field was furrow irrigated as needed. The soybean yield was measured and recorded at the time of harvest on September 9, 2014.

For early detection of soybean injury from low-dose dicamba, ASD Handheld 2 Portable Spectroradiometer (ASD Inc., Boulder, CO) was used to measure on the top of the soybean canopy at 24 HAT (Hours after Dicamba Treatment), 48 HAT and 72 HAT. For radiometric calibration the 0.3 m×0.3 m Spectrolon® white reference target with 99% nominal reflectance (Labsphere, North Sutton, NH) was used. In the field measurement, within each plot, three random points on plant canopy were measured with sensor optimization, white reference measurement and a dark current measurement.

Figure 4 shows the average percent reflectance curves of 0.0X, 0.05X and 0.1X at 24 HAT, 48 HAT and 72 HAT, respectively. From the curves it can be seen that regardless HAT they are differentiable at the wavelength of 550 nm, 673 nm and 800 nm, especially 0.0X from 0.1X.

The sensitive wavelengths of 550 nm, 673 nm and 800 nm are corresponding to narrow green band (Green), red band (Red) and near-infrared (NIR) band, respectively. With them, red normalized difference vegetation index (rNDVI) and green normalized difference vegetation index (gNDVI) can be calculated to characterize plant vigor and greenness, respectively, as:

$$rNDVI = \frac{NIR - Red}{NIR + Red} \text{ [16]} \quad (2)$$

$$gNDVI = \frac{NIR - Green}{NIR + Green} \text{ [17]} \quad (3)$$

Although the determination of the sensitive wavelengths is subjective, it is an effective and practical way to rapidly generate simple vegetation indices such as rNDVI and gNDVI.

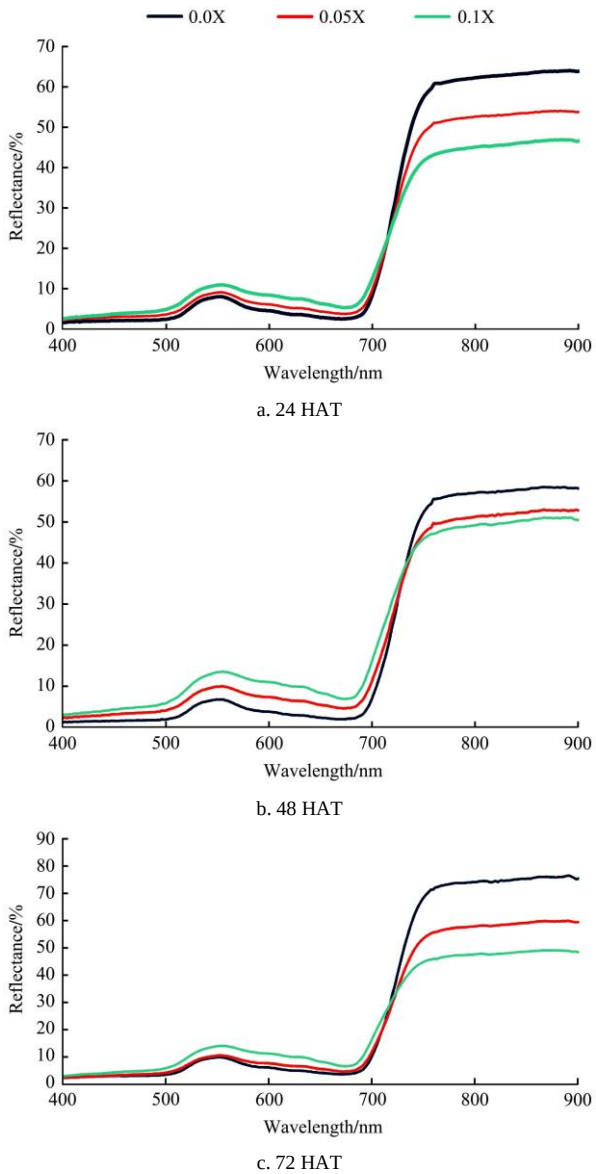

a. 24 HAT

b. 48 HAT

c. 72 HAT

Note: Sensitive bands: 550 nm (Green), 673 nm (Red), and 800 nm (NIR).

Figure 4 Average percent reflectance curves of 0.0X, 0.05X and 0.1X at 24 HAT, 48 HAT and 72 HAT, respectively

Table 1 shows rNDVI and gNDVI at 24, 48 and 72 HAT in 0.0X, 0.05X and 0.1X. The Duncan's multiple range tests at the confident level of 95% provide that in all the cases 0.0X is significant from 0.1X and at 72 HAT and gNDVI is significantly different in 0.0X, 0.05X and 0.1X.

Table 1 Duncan mean separation of rNDVI and gNDVI at different doses and HATs (α=0.05)

	rNDVI Reduction/%			gNDVI Reduction/%		
Dose \ HAT	24	48	72	24	48	72
0.0X	0[b]	0[b]	0[b]	0[b]	0[b]	0[c]
0.05X	6[ba]	11[b a]	6[b]	9[ba]	15[ba]	10[b]
0.1X	14[a]	19[a]	17[a]	20[a]	27[a]	28[a]

Note: Different letters mean significantly different.

The results indicated that rNDVI and gNDVI can detect soybean injury from dicamba at the low rate of 0.1X reliably at 24 HAT, 48 HAT, and 72 HAT at 95% confidence level, and hyperspectral remote sensing has a great potential in early detection of soybean injury from exposure to off-target dicamba drift in the field.

3.1.2 Laboratory hyperspectral imaging system for characterization of soybean injury from dicamba

Hyperspectral imaging provides an approach to assessing crop injury from different doses of dicamba, which simulates crop injury from off-target drift of dicamba. Compared to the method using ASD spectroradiometer, hyperspectral images can be used to separate the plant from the ground accurately to focus on the vegetation signatures of the healthy or injured crop. The study of hyperspectral imaging for assessing crop injury from dicamba started in 2012 yearly until 2014. The field of the study is in the 4.5 hm^2 field of USDA-ARS Crop Production Systems Research Farm in Stoneville, Mississippi, as mentioned above. The field was buffered by corn plants to prevent the vapor drift of dicamba from the neighboring fields. In each experimental area, 32 plots were planted. Each plot was eight rows with 0.97 m wide and 24 m long. In 2012, the field was planted cotton and soybean for experiments. However, the first field dicamba treatment could not be completed due to severe weather. The plants of the retreated field must be differentiated to extract useful information for the experiment. In 2013, with the lesson of 2012, in the east side of the field 32 plots were planted soybean (Pioneer 94Y90) on May 9 and in the west side of the field, as a backup, 32 plots were planted the same soybean on May 31. In 2014, the experiment was successful on the east side of the field so the backup field in west side was not used. In this research, the results of 2013 are presented.

On June 5, 2013, the east side of the field was treated with dicamba, but heavy thunder storms came on right after the treatment was completed. It was thus surmised that applied herbicide was washed out. Therefore, on July 1, when soybean was at the four-trifoliolate stage, the west side of the backup field was treated with dicamba at 0.0X (control), 0.05X, 0.1X, 0.2X, 0.3X, 0.5X and 1.0X, where X=0.56 kg ae/hm^2 of dicamba. Dimethylamine salt of dicamba, RIFLE® was applied using a tractor mounted sprayer with Tee Jet 4003 standard flat-spray nozzles delivering 140 L/hm^2 of water at 193 kPa. Each treatment (0.05X, 0.1X, 0.2X, 0.3X, 0.5X and 1.0X) was mixed with 57 L water and 150 ML induce adjuvant. No postemergence herbicides were applied up to 3 weeks after dicamba treatment for taking various measurements. Three weeks after dicamba treatment, other postemergence herbicides were applied as needed to keep the plots weed-free, and the field was furrow irrigated as needed.

After field treatment five soybean plants from each plot were randomly sampled in field and transported to laboratory for plant imaging using the lab settings of the Pika II hyperspectral imaging system at 1, 2, and 3 weeks after treatment (WAT). The white reference and dark current were measured daily before plant imaging or when the lighting condition in the lab significantly changed. The white reference target was the 0.3 m×0.3 m Spectrolon® white reference board with 99% nominal reflectance. The light source was a pair of 70 watt ASD quartz-tungsten-halogen illuminator reflectance lamps, as described previously.

Observation of the measured spectral curves indicated that, regardless HAT and X (dose), the curves were differentiable at the wavelength of 550 nm, 680 nm and 760 nm, which correspond to narrow green band (G), red band (R) and near-infrared (NIR) band, respectively. With the bands, rNDVI and gNDVI were calculated as indicated in Figure 5. From the figure, it can be seen that at 1 WAT, both NDVIs indicate a dose response of plants; gNDVI and rNDVI showed growth stimulus at low doses of 0.05X and 0.1X. At 2 WAT both indices indicated the death level of the plant starting at the dose of 0.2X. At 3 WAT both NDVIs indicated some

re-growth at high dose such as rNDVI at 1.0X. Results indicated that the spectral information extracted from hyperspectral imaging in lab settings can be used to assess soybean injury from different doses of dicamba in the field.

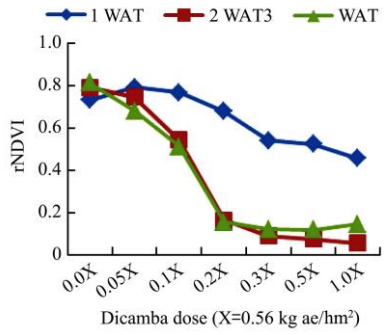

a. rNDVI

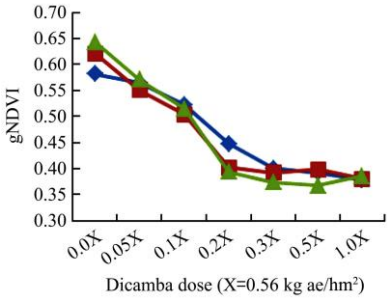

b. gNDVI

Figure 5 rNDVI and gNDVI calculated from Pika II hyperspectral images to assess soybean injury from different doses of dicamba in field

3.1.3 Field on-the-go hyperspectral imaging system for characterization of soybean injury from dicamba

For the study of 2013, at 1, 2 and 3 WAT after lab imaging, the Pika II system was mounted on a tractor to move over the field to image the soybean plants in each plot. There existed two issues during field imaging. One was sensor overheating under direct sun light, which resulted in the failure of imaging at 2 WAT. The other was wind disturbance, which resulted in deformation of leaves in the images due to mismatch of imaging line scan and leaf movement even with a very low wind. The solution of sensor overheating was to build a fan beside the imaging sensor to blow out the heat. Wind disturbance was minimized by shutting off the tractor and lengthening the distance from the sensor to the top of the soybean canopy to confine the wind effect within a pixel; image processing automatically segmented plant pixels from the soil background by thresholding each band with the green portion of the spectrum.

Due to the uncertainties in field imaging from weather and sensor system, the sensitive bands of the spectral curves changed from 550 nm, 680 nm and 760 nm in lab imaging to 565 nm, 691 nm and 735 nm in field imaging. Figure 6 shows that field imaging was closely related to lab imaging through rNDVI and gNDVI.

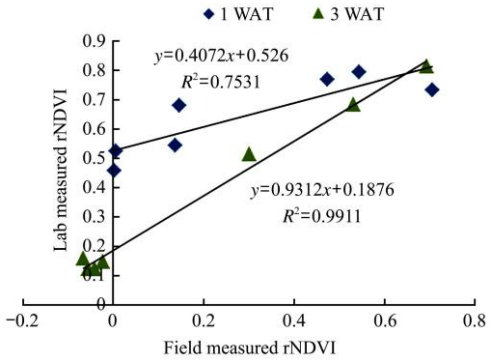

a

Note: y represents $rNDVI_L$ and x represents $rNDVI_F$.

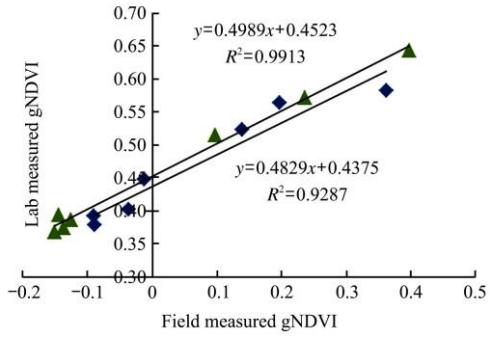

b

Note: y represents gNDVIL and x represents gNDVIF.

Figure 6 Correlation of lab measured rNDVI and field measured rNDVI (a) and lab measured gNDVI and field measured gNDVI

From 1 WAT to 3 WAT SNR (signal noise ratio) of rNDVI in lab increased from 1.86 to 22.47 while the SNR of gNDVI in lab only increased from 1.29 to 1.34. This indicated that 3 WAT was the best period for lab imaging used as a surrogate of field imaging, which is much less uncertain, through rNDVI. SNR was calculated as:

$$SNR \approx \frac{\Delta NDVI_F}{S} \quad (4)$$

where, $\Delta NDVI_F = (NDVI_{F,\max} - NDVI_{F,\min})$; $S = \sqrt{\frac{\sum_{i=1}^{n}(NDVI_{L,i} - NDVI_{F,i})^2}{n}}$ is the standard deviation of $NDVI_L$; NDVI is whatever rNDVI or gNDVI; NDVIL is the NDVI from lab imaging; NDVIF is the NDVI from field imaging; and n is the number of data points. It is important to note that Equation (4) assumes

that the true NDVI is measured in the lab with very high precision, and the difference between the lab measurement and field measurement generates the error. The precision of reflectance measurements obtained in the lab is extremely high, but in order to assure the accuracy, care must be taken to transport samples from the field to the lab and process them quickly; otherwise, the samples will begin to decay quickly[18,19].

3.2 Identification and characterization of glyphosate resistance of weeds

3.2.1 Laboratory hyperspectral imaging systems for characterization of glyphosate resistance of Palmer amaranth and Italian ryegrass

Repeated and intensive use of herbicide has exerted a high selection pressure on weed populations resulting in evolution of herbicide-resistance in weeds. Glyphosate [*N*-(phosphonomethyl) glycine], as the most widely used herbicide, has increased use in frequency and amount in the fields planted with genetically modified (GM) glyphosate-resistant (GR) crops such that repeated and intensive use of glyphosate has exerted a high selection pressure on weed populations resulting in evolution of GR weeds, such as GR Palmer amaranth, which was reported in 25 states in the United States[20], and GR Italian ryegrass, which was reported in seven states in the United States[9]. Both GR Palmer amaranth and GR Italian ryegrass are troublesome weeds in corn, cotton and soybean fields. GR Palmer amaranth can emerge throughout the growing season, grow rapidly, reaching heights in excess of 2 m, quickly overtopping crops such as cotton and soybean, and reduce yield and harvest efficiency. Italian ryegrass is an erect winter annual with a biennial-like growth habit. It grows vigorously in winter and early spring and is highly competitive. GR Italian ryegrass populations could seriously jeopardize preplant burndown options and planting operations in reduced-tillage crop production systems.

Not all weed field populations are resistant to glyphosate. GR and glyphosate-sensitive (GS) Palmer amaranth or Italian ryegrass look alike, and visually it is difficult to distinguish the GR plants from GS plants. The objective of this project is to develop hyperspectral imaging technology for rapid, consistent and accurate differentiation between GR and GS weeds from soybean field. The results could provide guideline data to allow crop producers and consultants to effectively identify GR weeds in crop fields for site-specific weed management.

The study was first conducted in greenhouse[21,22]. In greenhouse two groups of Palmer amaranth were planted consecutively in September-October 2012 and November-December 2012 for genetically heterogeneous (27 GS and 25 GR) and homogeneous (61 GS and 72 GR) plants, respectively. The genetically heterogeneous group was imaged at the 6-7 leaf growth stage and the genetically homogeneous group was imaged in the early flowering stage. Two hundred twenty six heterogeneous Italian ryegrass plants (119 GR, 107 GS) were grown and imaged twice at three and four weeks after emergence.

The Resonon Pika II hyperspectral camera mounted on a stand was used to capture images of the Palmer amaranth and Italian ryegrass planted in greenhouse. In image processing each percent reflectance image was segmented to separate the plant from the background by thresholding the band centered at 770 nm at 60% of the maximum value in the image. Plants typically reflect more light than soil in the near-infrared portion of the spectrum. The 770 nm band was chosen based on the tests providing acceptable segmentation. After image segmentation, all the pixels labeled as the plant were averaged to obtain a mean reflectance for each plant. The mean reflectance was then normalized to eliminate the effect of taller plants being exposed to higher light intensity. Normalization was accomplished by dividing each spectral value by the magnitude of square root of sum of all spectral values. Then, a subset of hyperspectral bands was chosen using a forward selection algorithm to optimize the area under the receiver operating characteristic (ROC) between GR and GS plants. The dimensionality of selected bands is reduced using linear discriminant analysis (LDA). Finally, the maximum likelihood classification was conducted for plant sample differentiation.

Results show that the images of Palmer amaranth determined 14 wavebands from within or near the regions of 400-500 nm, 650-690 nm, 730-740 nm and 800-900 nm for classification of unknown GR and GS plants

with an overall validation accuracy of 94% for greenhouse-grown plants (22 GS and 25 GR). The overall classification accuracy of unknown Italian ryegrass plants (27 GS and 30 GR) was 75% for the measurement, three weeks after emergence and 80% four weeks after emergence depending on the age of the plants.

3.2.2 Field on-the-go hyperspectral imaging systems for characterization of glyphosate resistance of Palmer amaranth

For field study[12] about 200 Palmer amaranth plants (100 GS and 100 GR) similar to the genetically heterogeneous group were grown in the greenhouse until they were 10-15 cm tall when 160 of them (80 GS and 80 GR) were transplanted into the experiment field in July 2013. The plants were imaged in early August 2013, when they were about 75-120 cm tall.

The Pika II hyperspectral camera used in the laboratory was adapted to mount on a three-point hitch on a tractor to allow flexible vertical and horizontal move to image the plants in the field. Imaging of each plant took about 3-4 min with image calibration by collecting white reference at the plant canopy. At the time of field imaging, the height of the plants varied from 75 cm to 120 cm so that the height of the camera was adjusted consistently to maintain the sensor at 66 cm above the top of crop canopy.

The image processing and analysis were performed similar to what have done for laboratory imaging. The 770 nm-based image segmentation algorithm was especially effective in processing field plant images acquired under rugged field conditions.

The results show that the images of Palmer amaranth also determined 14 wavebands from within or near the regions of 400-500 nm, 650-690 nm, 730-740 nm and 800-900 nm for classification of unknown GR and GS plants with an overall validation accuracy of 96% for field-grown plants.

3.3 Chlorophyll fluorescence signal extraction from hyperspectral images for characterization of crops and weeds

Fundamental vegetation characterization of remote sensing is based on spectral reflectance measurement of plant leaf or canopy. However, reflectance-based remote sensing has two drawbacks[23]. First, the spectral indices and features derived from reflectance data, such as rNDVI and simple ratio vegetation index (Red/NIR), are sensitive to low chlorophyll contents but tend to saturate at higher chlorophyll levels. Second, leaf reflectance spectra can reflect foliar optical properties, but give no insight into the biophysical status of plants. As compared to reflectance data, plant leaf chlorophyll fluorescence is closely related to the photosynthesis process and could be used as an indicator of the physiological state of plant[24,25].

The onset of soybean injury from glyphosate has been successfully detected[23] through analysis of chlorophyll fluorescence signal extracted from hyperspectral measurement of plant leaves using an ASD integrating sphere (ASD Inc., Boulder, Colorado) coupled with a non-imaging ASD FieldSpec 3 Hi-Res spectroradiometer (ASD Inc., Boulder, Colorado) and a removable filter for high-pass at 700 nm. The purpose of this study was to evaluate Pika II imaging system to image plants with spectral images to extract fluorescence signals. The evaluated system and methods will be prepared for further studies to characterize plant status.

The process of fluorescence signal extraction from hyperspectral images is described as follows. The spectral reflectance of the plants was imaged using the lab settings of the Pika II hyperspectral imaging system with a spectral resolution of 2.1 nm. The spectral images were collected in digital number (DN) mode and the plants in the images were segmented out from the background. Then, the spectral reflectance of the plant in each image can be calculated in average as:

$$R = \frac{DN_s - DN_d}{DN_w - DN_d} R_w \quad (5)$$

where, DN_s is the digital number of plant sample; DN_w is the digital number of white reference; DN_d is the digital number of dark current; and R_w is the reflectance of the white reference which was provided by the manufacturer (0.3 m × 0.3 m Spectrolon® white reference board, Labsphere, North Sutton, NH).

In order to extract fluorescence signals, the spectral reflectance of each plant was imaged the second time.

At this time, a filter was mounted on light source to limit the light going through it to illuminate the plant sample. Because the spectral range that can excite the chlorophyll fluorescence is from 400 nm to 700 nm, images with the long-pass filters in front of the light source should filter out the fluorescence signal. With the filter off, the reflectance spectrum as imaged and calculated with equation (4) contains the contribution of both the reflected radiance and chlorophyll fluorescence. The spectral reflectance with filter, R_f, can be similarly imaged and calculated with Equation (4). So, the chlorophyll fluorescence, *CF*, can be extracted through calculation as follows:

$$CF = (R - R_f) \times L_{rad} \quad (6)$$

where, L_{rad} is the radiance of the light source which is provided by the manufacturer (70 watt quartz-tungsten-halogen illuminator reflectance lamp, ASD Inc., Boulder, CO).

Figure 7 shows the light condition for imaging Italian ryegrass, as mentioned above that it is a weed that develops glyphosate resistance in crop fields, with and without a 650 nm long-pass filter in front of the light source. Figure 8 shows typical digital number curves used to calculate the reflectance with and without a 650 nm long-pass filter for Italian ryegrass. The fluorescence signal curve calculated from the difference of the two reflectances is also shown in the figure. The peaks in the fluorescence curve at 685 nm and 748 nm are critical features from the signal to characterize the status of the plant, species, vigor or stress.

a b

Figure 7 Pika II imaging Italian ryegrass without (a) and with (b) a 650 nm long-pass filter in front of the light source

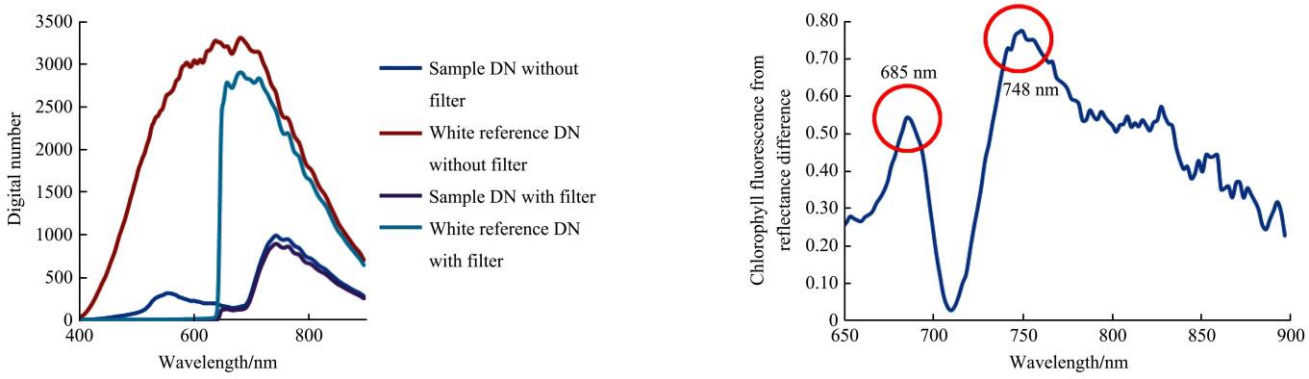

a b

Figure 8 (a) Digital number curves of Italian ryegrass sample and white reference with and without a 650 nm long-pass filter on light source (b) Chlorophyll fluorescence signal extracted from the data in (a)

4 Conclusions

Our studies indicated that GBHRS is versatile and effective for providing guiding data and information for precision weed management. The handheld hyperspectral radiometer is portable and effective for rapid, early detection of the onset of soybean injury from dicamba in the low spray rate within three days after treatment in field. The hyperspectral imaging system in laboratory under controlled illumination condition provided high-quality images for precision analysis of field soybean injury from dicamba with accurate crop

response to the doses of sprayed dicamba, high-accuracy differentiation of GR weeds from GS weeds with the accuracies from 75% to 95%, and extraction of chlorophyll fluorescence signals from plant spectra to develop innovative approach for advancement of the technology. The hyperspectral imaging system mounted on the tractor could collect on-the-go image data across the field for effective plant canopy spectral analysis, especially in field GR and GS weed differentiation with an over 90% accuracy, although the challenges exist from wind interference to sensor line scanning and sensor overheat under persistent sunshine.

The next studies for us will be to optimize the configurations of the laboratory and field systems to remove the data artifacts and minimize system and environmental interferences. The improved systems will be integrated to coordinate with low-altitude unmanned aerial remote sensing systems to provide timely and accurate information for field robots and herbicide application systems for effective weed management.

Acknowledgements

Thanks to Mr. David Fisher for his assistance in spectral measurement with the ASD handheld spectroradiometer in the soybean field. Thanks also to Mr. David Thornton, Mr. Earl Franklin, and Mr. Efren Ford for their assistance in the field.

[References]

[1] Lan Y, Huang Y, Martin D E, Hoffmann W C. Development of an airborne remote sensing system for crop pest management: System integration and verification. Applied Engineering in Agriculture, 2009; 25(4): 607–615.

[2] Huang Y, Thomson S J, Lan Y, Maas S J. Multispectral imaging systems for airborne remote sensing to support agricultural production management. International Journal of Agricultural and Biological Engineering, 2010; 3(1): 50–62.

[3] Huang Y, Sui R, Thomson S J, Fisher D K. Estimation of cotton yield with varied irrigation and nitrogen treatments using aerial multispectral imagery. International Journal of Agricultural and Biological Engineering, 2013; 6(3): 37–41.

[4] Yao H, Huang Y. Remote sensing applications to precision farming. In: G. Wang and Q. Weng, editors, Remote sensing of natural resources. Chap 18. CRC Press, Boca Raton, FL. 2013; p. 333–352.

[5] Huang Y, Thomson S J. Remote sensing for cotton farming. In: Cotton, 2nd edition, Eds. D. D. Fang and R.G. Percy. American Society of Agronomy, Inc., Crop Science Society of America, and Soil Society of America, Inc. Madison, WI, USA, Agronomy Monograph, 2015; 57: 1–26.

[6] Huang Y, Thomson S J, Hoffman W C, Lan Y, Fritz B K. Development and prospect of unmanned aerial vehicles for agricultural production management. International Journal of Agricultural and Biological Engineering, 2013; 6(3): 1–10.

[7] Lamb D W, Brown R B. Remote sensing and mapping of weeds in crops –a review of airborne remote sensing. Journal of Agricultural Engineering Research, 2010; 78(2): 117–125.

[8] Thorp K, Tian L. A review on remote sensing of weeds in agriculture. Precision Agriculture, 2004; 5(5): 477–508.

[9] Deng W, Huang Y, Zhao C, Wang X. Discrimination of crop and weeds on visible and visible/near-infrared spectrums using support vector machines, artificial neural network and decision tree. Sensors and Transducers, 2014; 26: 26–34.

[10] Deng W, Huang Y, Zhao C, Chen L, Meng Z. Comparison of SVM, RBF-NN, and DT for crop and weed identification based on spectral measurement over corn fields. International Agricultural Engineering Journal, 2011; 20(1): 11–19.

[11] Deng W, Huang Y, Zhao C, Wang X. Identification of seedling cabbages and weeds using hyperspectral imaging. International Journal of Agricultural and Biological Engineering, 2015; 8(5): 65–72.

[12] Huang Y, Thomson S J, Ortiz B V, Reddy K N, Ding W, Zablotowicz R M, Bright Jr. J R. Airborne remote sensing assessment of the damage to cotton caused by spray drift from aerially applied glyphosate through spray deposition measurements. Biosystems Engineering, 2010; 7: 212–220.

[13] Huang Y, Reddy K N, Thomson S J, Yao H. Assessment of soybean injury from glyphosate using airborne multispectral remote sensing. Pesticide Management Science, 2015; 71: 545–552.

[14] Huang Y, Thomson S J, Molin W T, Reddy K N, Yao H. Early detection of soybean plant injury from glyphosate by measuring chlorophyll reflectance and fluorescence. Journal of Agricultural Science, 2012; 4(5): 117–124.

[15] Yao H, Huang Y, Hruska Z, Thomson S J, Reddy K N. Using vegetative index and modified derivative for early detection of soybean plant injury from glyphosate. Computers and Electronics in Agriculture, 2012; 89: 145–157.

[16] Rouse J W, Haas R H, Schell J A, Deering D W. Monitoring vegetation systems in the great plains with ERTS.

Proc 3rd ERTS Symposium NASA SP-351, Vol. 1, NASA, Washington, DC, 1973; 309–317.

[17] Gitelson A A, Kaufman Y J, Merzlyak M N. Use of a green channel in remote sensing of global vegetation from EOS-MODIS. Remote Sens. Environ., 1996; 58: 289–298.

[18] Lee, M A, Huang, Y, Haibo, Y, Thomson, S J, Bruce, L M. Determining the effect of storage of cotton and soybean leaf samples for hyperspectral analysis. IEEE Journal of Selected Topics in Applied Earth Observations and Remote Sensing, 2014; 7(6): 2562–2570.

[19] Lee, M A, Huang, Y, Yao, H, Thomson, S J, Bruce, L M. Effects of sample storage on spectral reflectance changes in corn leaves excised from the field. Journal of Agricultural Science, 2014; 6(8): 214–220.

[20] Heap I M. International Survey of Herbicide Resistant Weeds. www.weedscience.org. Accessed on [2015-03-10].

[21] Reddy K N, Huang Y, Lee M A, Nandula V K, Fletcher R S, Thomson S J, Zhao F. Glyphosate-resistant and glyphosate-susceptible Palmer amaranth (*Amaranthus palmeri* S. Wats.): hyperspectral reflectance properties of plants and potential for classification. Pest. Manag. Sci. 2014; 70: 1910–1917. doi: 10.1002/ps.3755.

[22] Lee, M A, Huang, Y, Nandula, V K, Reddy, K N. Differentiating glyphosate-resistant and glyphosate-sensitive Italian ryegrass using hyperspectral imagery. In Sensing for Agriculture and Food Quality and Safety VI, Moon S. Kim; Kuanglin Chao, Editors, Proceedings of SPIE Vol. 9108 (SPIE, Bellingham, WA 2014), 91080B.

[23] Zhao F, Guo Y, Huang Y, Reddy K N, Zhao Y, Molin W T. Detection of the onset of glyphosate-induced soybean plant injury through chlorophyll fluorescence signal extraction and measurement. Journal of Applied Remote Sensing, 2015; 9(1): 1–12.

[24] Van der Tol C, Verhoef W, Rosema A. A model for chlorophyll fluorescence and photosynthesis at leaf scale. Agric. Forest Meteorol, 2009; 149: 96–105.

[25] Meroni M, Rossini M, Guanter L, Alonso L, Rascher U, Colombo R, Moreno J. Remote sensing of solar-induced chlorophyll fluorescence: review of methods and applications. Remote Sens. Environ, 2009; 113: 2037–2051.